Meteoritics & Planetary Science 37, xxx–xxx (2002)
Available online at http://www.uark.edu/meteor

Spaceborne ultraviolet 251–384 nm spectroscopy of a meteor during the 1997 Leonid shower

PETER JENNISKENS[1*], ED TEDESCO[2], JAYANT MURTHY[3†], CHRISTOPHE O. LAUX[4] AND STEPHEN PRICE[5]

[1]SETI Institute, 2035 Landings Drive, Mountain View, California 94043, USA
[2]TerraSystems, Inc., Space Science Research Division, 59 Wednesday Hill Road, Lee, New Hampshire 03824-6537, USA
[3]Department of Physics and Astronomy, The Johns Hopkins University, Applied Physics Laboratory, Baltimore, Maryland 21218-2686, USA
[4]High Temperature Gas Dynamics Laboratory, Building 520, Mechanical Engineering Department, Stanford University, Stanford, California 94305-3032, USA
[5]AFRL/VSB, 29 Randolf Road, Hanscom Air Force Base, Massachusetts 01731-3010, USA
[†]Present address: Indian Institute of Astrophysics, Koramangala, Bangalore 560 034, India
*Correspondence author's e-mail address: pjenniskens@mail.arc.nasa.gov

(Received 2002 March 18; accepted in revised form 2002 May 7)

Abstract–We used the ultraviolet to visible spectrometers onboard the midcourse space experiment to obtain the first ultraviolet spectral measurements of a bright meteor during the 1997 Leonid shower. The meteor was most likely a Leonid with a brightness of about –2 magnitude at 100 km altitude. In the region between 251 and 310 nm, the two strongest emission lines are from neutral and ionized magnesium. Ionized Ca lines, indicative of a hot $T \approx 10\,000$ K plasma, are not detected. The Mg and Mg^+ line intensity ratio alone does not yield the ionization temperature, which can be determined only by assuming the electron density. A typical air plasma temperature of $T = 4400$ K would imply a very high electron density: $n_e = 2.2 \times 10^{18}$ m^{-3}, but at chondritic abundances of Fe/Mg and Si/Mg ≈ 1. For a more reasonable local-thermal-equilibration (LTE) air plasma electron density, the Mg and Mg^+ line ratio implies a less than chondritic Fe/Mg = 0.06 abundance ratio and a cool non-LTE T = 2830 K ionization temperature for the ablation vapor plasma. The present observations do not permit a choice between these alternatives. The new data provide also the first spectral confirmation of the presence of molecular OH and NO emission in meteor spectra.

INTRODUCTION

Most normal meteor emissions at visible and near-infrared wavelengths during peak brightness originate from a relatively cool plasma with a typical excitation temperature of ~4000 K (Ceplecha, 1973; Borovicka *et al.*, 1999; Borovicka and Jenniskens, 2000; Jenniskens *et al.*, 2000a). This plasma is in quasi-local thermodynamic equilibrium with similar temperatures derived from electronic transitions of N, the vibrational structure of N_2, the chemical equilibrium of N, N_2 and O, and the relative intensity of line emission from meteoric metal atoms Mg I and Fe I (Jenniskens *et al.*, 2000a; Abe *et al.*, 2000). The emissions are now thought to originate mostly from a warm plasma in the wake of the meteoroid (Jenniskens *et al.*, 2000a; Boyd, 2000).

Additionally, a hot $T \approx 10\,000$ K component has been detected in meteor spectra, of which the most well-known emissions are the ionized Mg II line at 448.2 nm, the ionized Fe II lines at 458.4 and 501.8 nm, the Ca II doublet at 393.4 and 396.8 nm, the Si II lines at 634.9 and 637.3 nm, as well as the neutral H I lines at 656.4 and 486.3 nm (Brönshten, 1983; Borovicka, 1993, 1994a,b; Borovicka and Bocek, 1995; Borovicka and Betlem, 1997). These emission lines progressively increase in intensity with meteor brightness compared to those from the cooler gas within a single meteor (Cook and Millman, 1954; Harvey, 1971; from the Ca II/Mg I ratio) and with larger Leonid meteoroid mass (Borovicka *et al.*, 1999; from the Mg II/Mg I line ratio). The source of these emissions remains unknown, although it has been postulated that it is the cloud of meteoric vapor surrounding the meteoroid (Jenniskens *et al.*, 2000a; Popova *et al.*, 2000).

The temperature of the hot gas can be measured from the relative intensity of Mg II lines at 280 and 448 nm. Figure 1 shows the Mg II energy diagram. The 448 nm emission originates from much higher energy levels than the 280 nm emission. The latter, unfortunately, is only observable outside of Earth's atmosphere. Meisel (1976) did a study that considered many aspects of meteor ultraviolet spectroscopy from Earth orbit, but such an experiment was not realized until now.

In an earlier paper (Jenniskens *et al.*, 2000b), we reported the successful deployment of the ultraviolet imagers and imaging spectrometers (UVISI) spectrometer onboard the

Prelude preprint MS#4793

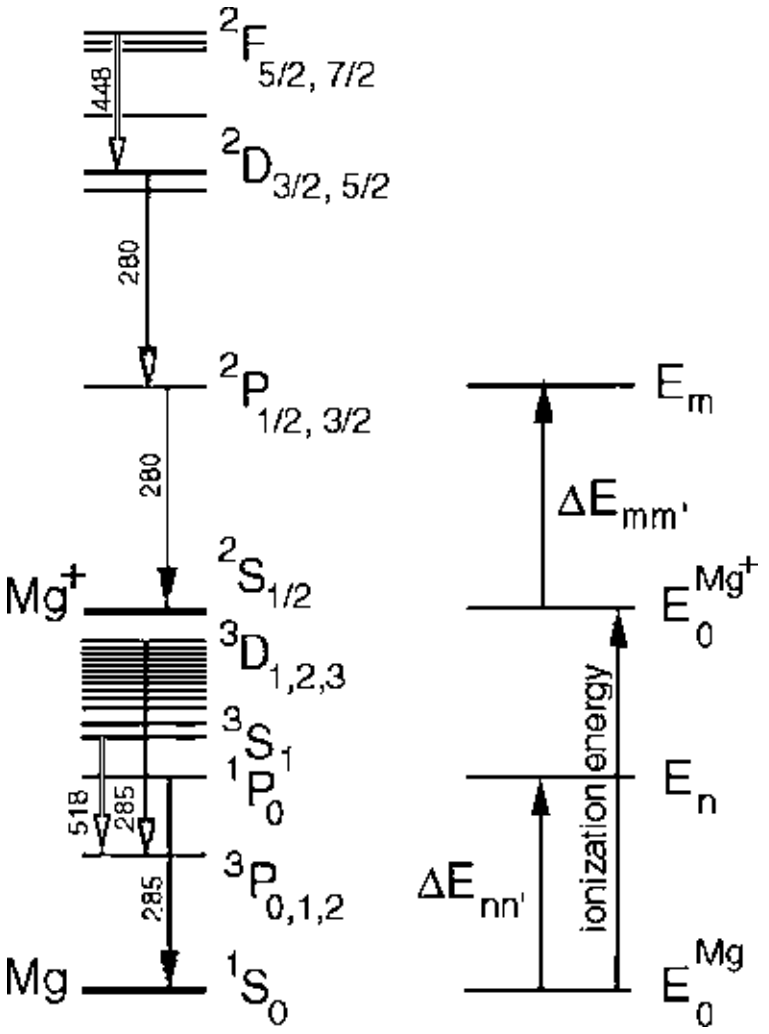

FIG. 1. Energy level diagrams for neutral and ionized magnesium atoms. Transitions discussed in the text are marked.

midcourse space experiment (MSX) satellite during the 1997 Leonid shower. A total of 29 meteors were detected near the limb of the Earth by the wide-field visible camera, and three by the narrow field visible camera, in a 48 min observing interval. Additionally, one meteor spectrum was recorded. Here we report on the analysis and interpretation of that spectrum. We have detected Mg^+ at 280 nm, but find the line much weaker than expected. We conclude that this emission originates from the warm plasma rather than from the hot component. This makes the 280 nm Mg^+ line a unique probe of the ionization conditions in the warm gas.

OBSERVING STRATEGY

The MSX satellite includes the first hyperspectral imagers flown in space, providing a unique capability for ultraviolet spectroscopy over a wide spectral range (Mill *et al.*, 1994; Hefferman *et al.*, 1996). The Johns Hopkins University, Applied Physics Laboratory developed, integrated, and operated MSX and built and operated the sensor suite of UVISI. This instrument suite consists of nine optical sensors, which are precisely aligned so transient events are viewed simultaneously. The multiple sensors cover the wavelength range from the ultraviolet L_α line to the far red. The sensor suite includes five spectrographic imagers (SPIMs) that span the wavelengths from 110 to 900 nm simultaneously at a sensitivity of 1–5 photons/ cm^2 s. The SPIMS wavelength range is divided into five regimes: 110–170 nm, 162–252 nm, 251–384 nm, 378–584 nm, and 580–893 nm, SPIM 1 to SPIM 5, respectively. The spectrographs have 272 × 40 pixel (charge-coupled device) CCD array sensors, which are downloaded with no compression at a rate of 2 Hz. Wide and narrow-field images are recorded simultaneously. Unfortunately, all nine data sets are not always obtained for each record, because of limitations set by the data transmission rate.

In deploying UVISI, we take into account that meteors are transient phenomena with highest apparent spatial density near the limb of the Earth. The viewing geometry for the experiment

was to have the spectrographs look to the night-time limb of the Earth in the anti-Sun direction. The Moon was full, but did not interfere with the observations. The slit was placed parallel to the Earth's surface at all times, taking into account the curvature of the Earth. The 0.1° slit width was used. An internal divert mirror steps the field across 1° vertical motion in ten 0.1° increments. This stepped the spectrometer field of view through an altitude range between 120 and 80 km in 4 km increments. In the 272×40 configuration, the cross-slit spatial resolution was 0.025°. Each individual exposure records the signal in an area 40 km wide and 1.4 km high (at the distance of 3300 km to the Earth's limb).

The observing period was chosen to be within the 2 h interval centered on 13:34 U.T., 1997 November 17, (day 321), when the Earth passed the orbital plane of comet 55P/Tempel–Tuttle (Yeomans *et al.*, 1996). Actual observations were not started until 14:28 U.T. The observations described here were obtained when the sensors looked into the side of the Earth facing the Leonid shower, at a time when the Leonids were falling perpendicular in projection in the Earth's atmosphere. This time was also close to the peak of the Leonid influx at 14 ± 3 h U.T. That shower was a recurrence of the "Leonid Filament" component with peak zenith hourly rate 70 meteors/h and bright meteors at a rate orders of magnitude above that from the sporadic background (Arlt and Brown, 1998; Jenniskens and Betlem, 2000).

RESULTS

When the meteor crosses the slit, a brief transient spectrum is recorded on top of a background spectrum from the natural airglow. A complete examination of the SPIM data shows that one meteor spectrum was obtained at 15 h 18 m 11 s U.T. (first of two 0.5 s files marked 15.3031). This occurred in the middle of the observing period between 15 h 12 m and 15 h 58 m U.T. Data from the wide-field imager and all five SPIMs are available for that time. Unfortunately, the noisy wide-field image does not show the meteor and there is no narrow-field image at this time. Hence, the brightness and the direction of motion of the meteor are unknown.

The meteor spectrum is identified as such because it is an emission line spectrum and, unlike stellar spectra, it is not seen in adjacent scans. Only the three long wavelength SPIMs show this transient signal. SPIM 4 and 5 cover the visual range. The spectra were extracted by averaging the rows with signal and subtracting an average of the remaining rows in the spectrum (Fig. 2). The wavelength scale was calibrated with a small linear correction. No correction for spectral response was needed, with all wavelength bandpasses having nearly constant response. The typical lines of Mg I, Na I, O I, and the first positive bands of N_2 from the warm plasma component are readily recognized (*e.g.*, Millman, 1980; Borovicka *et al.*, 1999). Most significantly, the emission lines of the hot Ca^+ at 393.5 and 397.0 nm are not detected. Two gaps in the meteor spectra of Fig. 2 are due to saturated emissions from the natural airglow background, specifically the molecular O_2 emission, which next to the meteoric O I line, and strong atmospheric green line emission at 557 nm (O I) next to the meteoric 517 nm Mg I emission. The numerous bands of OH in the airglow spectrum, as well as sodium emission, are subtracted out of the final spectrum, as well.

SPIM 3 shows, for the first time, an ultraviolet meteor spectrum at wavelengths below 384 nm, extending to 251 nm (Fig. 3). The spectral resolution is ~1.5 nm full width at half-maximum (FWHM). Several intense emission lines are

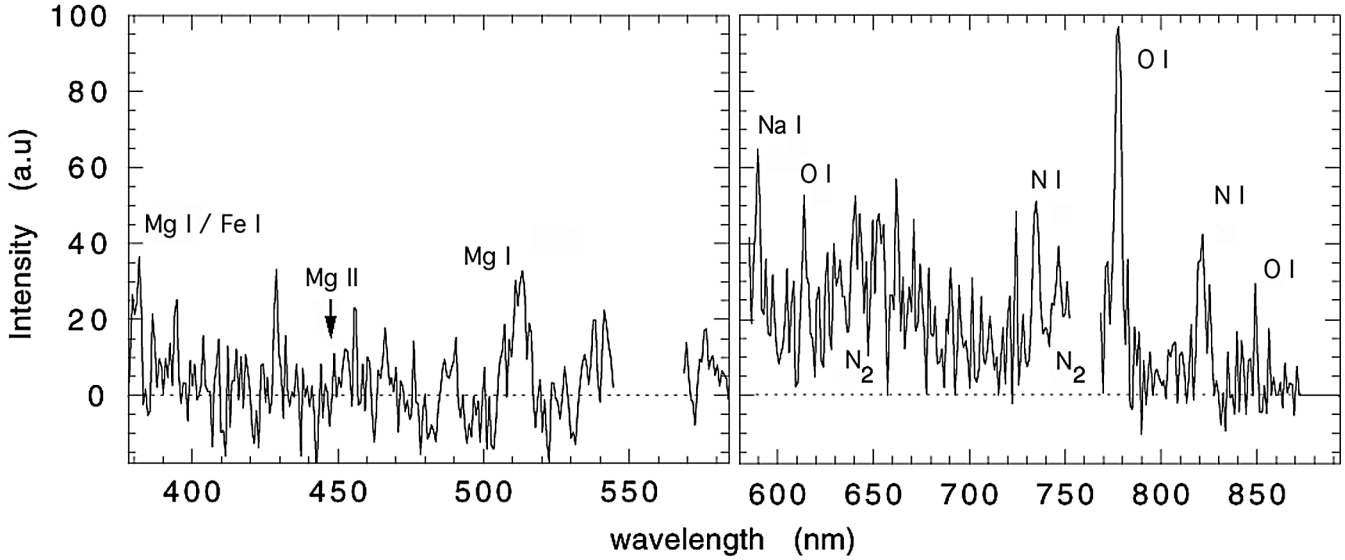

FIG. 2. Visible and near-infrared meteor spectrum from SPIM 4 (right) and SPIM 5 (left). Characteristic meteoric ablation lines of Fe I, Mg I and Na I are detected, as well as meteor-induced air plasma lines of O I, N I and molecular N_2.

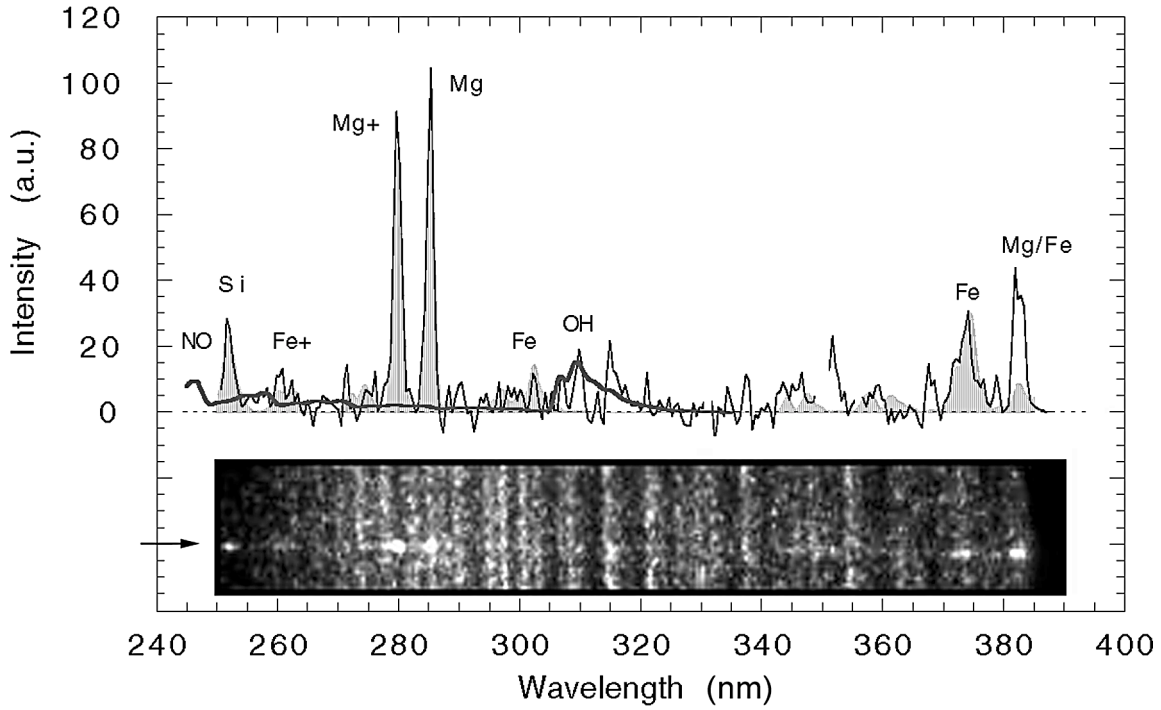

FIG. 3. The meteor spectrum in SPIM 3 is superposed on background OH airglow. The extracted spectrum is shown as a solid line and is superposed on a shaded contour, which is the theoretical spectrum for an LTE T = 4400 K and $P = 10^{-6}$ atm plasma, with chondritic metal atom abundances [Fe]/[Mg] = 0.52 and [Si I]/[Mg] = 0.82. Contours for NO (β and γ) and OH (A-X) under the same conditions are also shown with thick line, but with each molecule's abundance scaled to match the spectrum.

observed between 250 and 290 nm (Table 1). The central pixels are saturated and blooming is observed. Until now, ground- and aircraft-based observations have only been able to probe meteor spectra down to ~310 nm, which is sufficient to confirm the dominant presence of groupings of Fe I lines ~370 nm in the SPIM 3 spectrum (Halliday, 1969; Rairden *et al.*, 2000).

In order to identify the other spectral lines, we constructed synthetic meteor spectra following Borovicka and Jenniskens (2000). We consider an optical thin local-thermal-equilibration (LTE) plasma with emission line intensity given by:

$$I_{ij} \approx g_i/g_o \, E_{ij} \, A_{ij} \exp(-E_{io}/kT) \qquad (1)$$

where E_{ij} is the energy level difference between levels i and j of the transition, while E_{io} is the energy level of the upper state. The atomic transition probabilities for spontaneous emission A_{ij}, as well as electronic degeneracy factors g (= 2J + 1), can be found in the Harvard-Smithsonian Center for Astrophysics Kurucz Atomic Line Database (Kurucz and Bell, 1995). For each element, relative line intensities are calculated using a FWHM of 1.5 nm to mimic the MSX observations and T = 4400 K. The result for each element in each ionization state is matched to the data and the best fitting result is shown as a dashed line in Fig. 3. The strong lines of Mg I, Si I and Mg II are the most intense in the observed spectra. There are also unresolved groupings of Fe I and Fe II lines.

From air plasma studies with trace water, we expected also to see the molecular band emissions from NO γ (0,3), the second positive band of N_2, and if sufficient water is present perhaps also OH A-X (0-0) (Park *et al.* 1997, 1998). Indeed, the NO band may be responsible for a continuum below 290 nm, which is best seen ~256 nm (Fig. 3).

If so, the NO intensity is a factor of 20 less than expected for an LTE air plasma in relation to the strength of the first positive band of N_2 at 630 nm. The second positive band of N_2 at ~336 nm remains undetected and is at least a factor of 10 weaker than expected. There is emission at the position of OH, substantiating the reported two-channel photometric measurements of emission at this wavelength in Perseid and alpha-Capricornid spectra by Harvey (1977). However, the data are noisy and there can be potentially large residuals arising from the imperfect subtraction of the background airglow (Fig. 3). Taken at face value, the OH abundance is ~$10^5\times$ larger than expected for an LTE air plasma at 4400 K, even if the water content in the air at 100 km is a high 20 ppm. The expected value is <1 ppm (Conway *et al.*, 1999; Stevens *et al.*, 2001). We conclude that if this emission is due to OH, then the OH is not in chemical equilibrium and/or cometary meteoroids contain significant amounts of water in some form. Better data are needed to warrant further discussion.

The comparison between the strong O I lines and N_2 first positive bands and the metal atom line emissions of Mg and

TABLE 1. Ultraviolet meteoric emission lines identified in the spectrum.*

Wavelength (nm)		Identification Element (multiplet)	Σ Intensity (arbitrary units)	Notes
Measured	Theory			
252.1	251.8	Si I (U1)	105	Narrow, single line
~256	257.0	NO γ (0,3)	<40	Broad band
261.1	261.4	Fe II (U1)/NO ?	96	Blend of many lines
279.9	279.8	Mg II (U1)	280	Blend of two lines
285.2	285.2	Mg I (U1)	290	Narrow, single line
298	296–301	Fe I (9-11)	100	Weak blend
309.4	308	OH (A-X)	54	Band head
314.7	(311)	OH (A-X)	98	Band tail
321.9	319.2	Fe I (7,8)	55	Tentative, blend
350.0	347	Fe I (6)	150	Blend
373.3	373.0	Fe I (5)	240	Blend
381.6	382.0	Mg I (3), Fe I (4),	190	Blend

*Line intensities are integrated over the line profile.

Na, identify the spectrum as that of a fast meteor >40 km/s (Borovicka, 2001). Slower meteors tend to have relatively weaker air plasma lines. Fainter meteors are the more frequent and, if the observed spectra are from a Leonid (at 71 km/s), then the absence of the Ca II doublet in Fig. 2 implies an absolute magnitude (*i.e.*, when seen from a distance of 100 km) of less than $M_V = -4$ magnitude (see Rairden *et al.*, 2000). Indeed, fainter meteors are more frequent and the most likely meteor captured is one near the detection limit. This is consistent with the lack of a detection of the event in the wide-field imager. The limiting magnitude for limb observations of Leonid meteors by this instrument was measured to be $M_V = -1.5$ magnitude, but the sensitivity is less near the position in the image where the slit is positioned (Jenniskens *et al.*, 2000b). We conclude that this meteor was relatively faint, of magnitude $M_V = -2 \pm 2$ (apparent brightness $+5 \pm 2$). A Leonid of such brightness is first detected at ~110 km and seen to penetrate to 88 km in photographic observations (Jenniskens *et al.*, 1999). Indeed, the spectrum was taken when the slit was pointed at an altitude of 100 km.

DISCUSSION

Are the Magnesium I and Magnesium II Emissions from the Same Local-Thermal-Equilibration Plasma?

The Mg^+ line is relatively weak, which leaves no room for a strong contribution from a hot component (see below). The lack of the sensitive Ca^+ lines is also indicative that no hot component is present in the spectrum. That makes the sensitive 280 nm Mg^+ line a unique probe of the ionization conditions in the warm meteor plasma.

Let us assume that the excited states of Mg I are in Saha equilibrium with the electronic states of Mg II. The underlying assumption is that collisions between Mg I, Mg II, and electrons are sufficiently fast that the following quasi-equilibrium relation holds:

$$\mathrm{Mg}\,(n) + \mathrm{e} \;\Leftrightarrow\; \mathrm{Mg}^+\,(m) + \mathrm{e} + \mathrm{e} \qquad (2)$$

where n and m are indices that indicate the specific excited level responsible for the observed emissions. The emissions occur rapidly after excitation and most of the excitations occur from the ground state (Fig. 1). In case of equilibrium, the line ratio follows from the population density distribution, given by the Saha equation (*e.g.*, Nishikawa and Wakatani, 2000):

$$\frac{[\mathrm{Mg}+(m)][\mathrm{e}]}{[\mathrm{Mg}(n)]} = \frac{g^{\mathrm{Mg}^+}(m)\ \exp(-E_m/kT)}{g^{\mathrm{Mg}}(n)\ \exp(-E_n/kT)} \times 2 \times \left(2\pi m_\mathrm{e} kT/h^2\right)^{3/2}\ \exp(-\Delta E_\mathrm{o}/kT) \qquad (3)$$

where m_e is the electron mass, k the Boltzman constant, and h the Planck constant. $\Delta E_o = E_o^{Mg+} - E_o^{Mg} = 7.646$ eV is the ionization energy for magnesium. If more levels contribute to an observed transition, then the partition function is a summation over the upper levels that contribute to the observed emissions.

The relative abundance of Mg in the observed excited state [Mg (n)] follows directly from the observed line intensity (I), leaving the electron density as a free parameter. The total power radiated in a spectral line is given by:

$$I^{\mathrm{Mg}}(n) = \text{constant} \times [\mathrm{Mg}\,(n)]\ \Delta E_{nn'}\, A_{nn'} \qquad (4)$$

$$I^{Mg+}(m) = \text{constant} \times [Mg^{+}(m)]\, \Delta E_{mm'}\, A_{mm'} \qquad (5)$$

The constant is a characteristic of the detection system (spectral bandpass, intensity response, collection angle, detector area) and is equal for both equations if (1) the source region and detection conditions are the same, and (2) the spectral response of the detection system is identical at the wavelengths of the two transitions (which holds in the present case since the two lines are at approximately the same wavelength). The relevant transitions are identified in Fig. 1. Contributions from higher level states at nearly the same wavelength are found to be negligible, because of the comparatively lower population in these higher levels.

From Eqs. (3–5) and the measured line intensity ratio at 280 and 285 nm of $I^{Mg+}/I^{Mg} = 0.96 \pm 0.09$, we can calculate an electron density (m^{-3}) for each assumed temperature T (K):

$$[e] = 5.37 \times 10^{21}\, T^{1.5}\, \exp(-89624/T) \qquad (6)$$

The same approach for the Fe II band at 262 nm and the Fe I band at 372 nm gives a second relationship between [e] and T:

$$[e] = 3.68 \times 10^{23}\, T^{1.5}\, \exp(-108230/T) \qquad (7)$$

Both of the observed ion/neutral ratio's agree with the parameters: $T = 4400 \pm 250$ K and $[e] = 2.2 \times 10^{18}$ m^{-3}. This electron density is ~20% of the air density at ambient pressure and temperature! The metal ionization fraction is $[Mg^{+}]/[Mg] = 2.6 \pm 0.6$, while $[Fe^{+}]/[Fe] = 1.0 \pm 0.4$ (which is in good agreement with the expected value of ~1.3). The calculated abundance ratio is $[Fe]/[Mg] = ([Fe]+[Fe^{+}])/([Mg]+[Mg^{+}]) = 0.52 \pm 0.12$, in good agreement with the ratio of 0.52 for bulk chondritic CI-type composition (Rietmeijer and Nuth, 2000). Note that no information is available about the Si II abundance in the observed spectra. However, the ionization potential of Si is 8.15 eV, from which the ionization fraction is calculated as [Si+]/[Si] = 0.70. From this, we infer that $[Si]/[Mg] = 0.82 \pm 0.24$, in good agreement with the CI abundance ratio of 0.94. Apart from the unusually high electron density, the only other discrepancy is the mismatch for the 382.5 nm Mg I line, which is much stronger than calculated by a factor of 80, for which we have no explanation. However, Rairden *et al.* (2000) rejects the possibility that the feature is due to Fe.

The expected electron density for air plasma in LTE at 4400 K at the ambient pressure is 2.2×10^{-4} per mole (Fig. 4) or 2.7×10^{15} m^{-3}, 3 orders of magnitude lower than predicted by Eqs. (6) and (7). On the other hand, a –2 magnitude Leonid meteor at 100 km altitude is expected to have an electron line density of order $q = 1.1 \times 10^{17}$ m^{-1} based on radar reflection intensities (McKinley, 1961). Indeed, initial train radius theory predicts dimensions of the luminous plasma of $r_i = 2.4$ m, formed after ~10 collisions at 3×10^{-4} s (Jones, 1995). That translates into a similar low electron density of 6.2×10^{15} m^{-3}.

Can the extra electrons originate from the metal atoms? Immediately behind the meteoroid, the meteoric vapor density falls off to ~2×10^{17} m^{-3} (Boyd, 2000). Hence, even if a significant fraction of this material is ionized, there cannot be enough electrons to account for the high apparent electron density measured. Moreover, the measured ionization fractions exclude the dominant presence of even higher ionization states.

One way to lower the electron line density is to assume that the metal atom plasma is not in LTE and the ionization

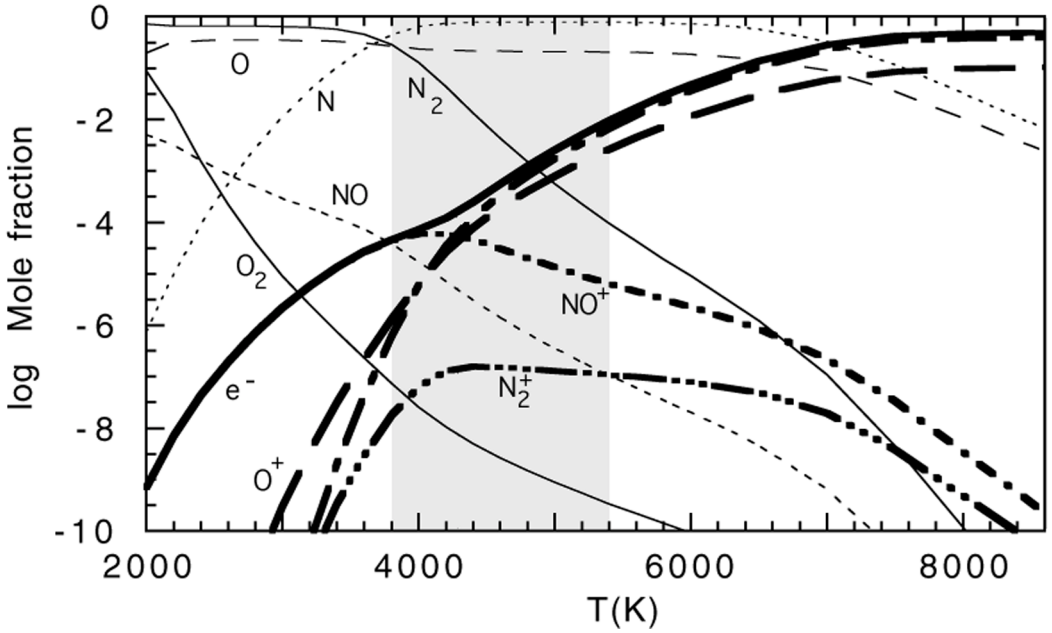

FIG. 4. Air plasma model thermodynamic equilibrium species concentration in pure air at 95 km altitude ($P = 0.0991$ Pa, 79% N_2, 21% O_2). Ionized components are shown in bold, which account for the total electron density shown as a solid line. Adapted from Jenniskens *et al.* (2000).

temperatures are less than the air plasma temperature. Indeed, if the Fe II lines are a factor of 10 weaker than assumed, the observed Mg and Fe ionization ratios are in agreement for an excitation temperature of $T = 2830$ K. In that case, the measured ionization ratio for magnesium comes out slightly higher, at $[Mg^+]/[Mg] = 3.2$. The inferred iron ionization fraction $[Fe^+]/[Fe] = 4.2$ is higher than that of magnesium, which can not be true. The expected ratio of ~1.6 implies that only 30% of the 261 nm feature is due to Fe^+. The remainder could be due to the NO γ (0,3) band. However, in that case the iron abundance would come out significantly lower than chondritic, with $[Fe]/[Mg] = 0.06$. Additionally, the derived silicon abundance is higher, at $[Si]/[Mg] = 2.3$.

A contribution from a hot plasma would decrease the available Mg^+ emission from the cold component, which would demand an even lower ionization temperature for Mg^+ and increase the discrepancy with Fe. Indeed, the observations show no evidence of a hot gas component.

A very high electron density could provide a partial explanation for the $10^5\times$ higher than expected O I 777 nm line intensity measured earlier by Jenniskens *et al.* (2000a). However, this solution also raises numerous questions about the physical conditions in meteor plasmas and, for example, the possible chemistry of released organic compounds at the time of the origin of life. Before addressing such issues, future spectroscopic studies need to make clear if this solution is more acceptable than the one with lower electron density and a cooler non-LTE temperature.

The spectrum discussed in this paper reveals that, as suspected but not previously observed, meteors do indeed emit spectral lines in the ultraviolet. This paper also shows that such spectra are bright enough to be observed from space with a relatively small instrument. This means that it is feasible to fly an inexpensive dedicated mission to observe such features. Future observations may be able to measure the ultraviolet and visible Mg^+ emissions simultaneously in brighter Leonid meteors to determine the hot plasma temperature, and obtain more precise measurements of the molecular NO and OH bands for quantitative analysis. Such experiments should also gather independent observations of the integrated visible brightness of the meteor and its speed and direction of motion for stream classification. Another essential datum would be the distance to the meteor. In this work, we chose to view the horizon, as it yielded the maximum number of incoming meteors per unit time per unit area. Unfortunately, this choice also produces the greatest uncertainty on the distance to the observed plasma.

This work demonstrates the need to understand the meteoric entry processes in much greater detail when obtaining ultraviolet spectra of meteors may become routine. Meteor spectra are a rich and largely untapped source of information on small bodies in the solar system, and it makes sense to derive as much information as possible from a resource that comes to us directly from known sources that may never be visited by a planetary spacecraft.

Acknowledgement–We thank referees Jiri Borovicka and Joseph Nuth for helpful comments. This work is supported in part by NASA's Exobiology and Astrobiology Programs. Support for MSX observing time and data handling was made available by AFRL/VSBC at Hanscom AFB and APL/John Hopkins University.

Editorial handling: A. Cochran

REFERENCES

ABE S., YANO H., EBIZUKA N. AND WATANABE J-I. (2000) First results of high-definition TV spectroscopic observations of the 1999 Leonid meteor shower. *Earth, Moon Planets* **82–83**, 369–377.

ARLT R. AND BROWN P. (1999) Visual results and modeling of the 1998 Leonids. *WGN, J. IMO* **27**, 267–285.

BOROVICKA J. (1993) A fireball spectrum analysis. *Astron. Astrophys.* **279**, 627–645.

BOROVICKA J. (1994a) Two components in meteor spectra. *Planet. Space Sci.* **42**, 145–150.

BOROVICKA J. (1994b) Line identification in a fireball spectrum. *Astron. Astrophys.* **103 (Suppl.)**, 83–96.

BOROVICKA J. (2001) Video spectra of Leonids and other meteors. In *Proceedings of the Meteoroids 2001 Conference*, pp. 203–208. Swedish Institute of Space Physics, Kiruna, Sweden.

BOROVICKA J. AND BETLEM H. (1997) Spectral analysis of two Perseid meteors. *Planet. Space Sci.* **45**, 563–575.

BOROVICKA J. AND BOCEK J. (1995) Television spectra of meteors. *Earth, Moon Planets* **71**, 237–244.

BOROVICKA J. AND JENNISKENS P. (2000) Time resolved spectroscopy of a Leonid fireball afterglow. *Earth, Moon Planets* **82–83**, 399–428.

BOROVICKA J., STORK R. AND BOCEK J. (1999) First results from video spectroscopy of 1998 Leonid meteors. *Meteorit. Planet. Sci.* **34**, 987–994.

BOYD I. D. (2000) Computation of atmospheric entry flow about a Leonid meteoroid. *Earth, Moon Planets* **82–83**, 93–108.

BRÖNSHTEN V. A. (1983) Luminosities and spectra of meteors. In *Physics of Meteor Phenomena*. D. Reidel, Dordrecht, The Netherlands. 165 pp.

CEPLECHA Z. (1973) A model of spectral radiation of bright fireballs. *Bull. Astron. Inst. Czech.* **24**, 232–242.

CONWAY R. R., STEVENS M. H., BROWN C. M., CARDON J. G., ZASADIL S. E. AND MOUNT G. H. (1999) The middle atmosphere high resolution spectrograph investigation. *J. Geophys. Res.* **104**, 16 327–16 348.

COOK A. F. AND MILLMAN P. M. (1954) Photometric analysis of a spectrogram of a Perseid meteor. *Contrib. Dominion Observatory* **2**, 250–270.

HALLIDAY I. (1969) A study of ultraviolet meteor spectra. *Publ. Dominion Observatory Ottawa* **25**, 313–322.

HARVEY G. A. (1971) The calcium H- and K-line anomaly in meteor spectra. *Astrophys. J.* **165**, 669–671.

HARVEY G. A. (1977) A search for ultraviolet OH emission from meteors. *Astrophys. J.* **217**, 688–690.

HEFFERMAN K. J., HEISS J. E., BOLDT J. D., DARLINGTON E. H., PEACOCK K., HARRIS T. J. AND MAYR M. J. (1996) The UVISI instrument. *Johns Hopkins APL, Technical Digest* **17**, 199–214.

JENNISKENS P. AND BETLEM H. (2000) Massive remnant of evolved cometary dust trail detected in the orbit of Halley-type comet 55P/Tempel–Tuttle. *Astrophys. J.* **531**, 1161–1167.

JENNISKENS P., DE LIGNIE M., BETLEM H., BOROVICKA J., LAUX C. O., PACKAN D. AND KRUGER C. H. (1999) Preparing for the 1998/99 Leonid storms. In *Laboratory Astrophysics and Space Research*. (eds. P. Ehrenfreund *et al.*), pp. 425–455. Kluwer Academic Publishers, The Netherlands.

JENNISKENS P., LAUX C. O., PACKAN D. M., WILSON M. AND FONDA M. (2000a) Meteors as a vector for the delivery of organic matter to the early Earth. *Earth, Moon Planets* **82–83**, 57–70.

JENNISKENS P., NUGENT D., TEDESCO E. AND MURTHY J. (2000b) 1997 Leonid shower from space. *Earth, Moon Planets* **82-83**, 305–312.

JONES W. (1995) Theory of the initial radius of meteor trains. *Mont. Not. R. Astron. Soc.* **275**, 812–818.

KURUCZ R. L. AND BELL B. (1995) *1995 Atomic Line Data, No. 23*. Smithsonian Astrophysical Observatory, Cambridge, Massachusetts (CD-ROM).

MCKINLEY D. W. R. (1961) *Meteor Science and Engineering*. McGraw-Hill Book Company, New York, New York. 309 pp.

MEISEL D. D. (1976) *A Study of Meteor Spectroscopy and Physics from Earth-Orbit: A Preliminary Survey into Ultraviolet Meteor Spectra*. NASA Contractor Report, NASA CR-**2664**. 82 pp.

MILL J. D., O'NEIL R. R., PRICE S. D., ROMICK G. J., UY O. M., GAPOSCHKIN E. M., LIGHT G. C., MOORE W., JR., MURDOCK T. L. AND STAIR A. T., JR. (1994) Midcourse space experiment: Introduction to the spacecraft, instruments, and scientific objectives. *J. Spacecraft Rockets* **31**, 900–907.

MILLMAN P. (1980) One hundred and fifteen years of meteor spectroscopy. In *Solid Particles in the Solar System* (eds. I. Halliday and B. A. McIntosh), pp. 121–128.

NISHIKAWA K. AND WAKATANI M. (2000) *Plasma Physics, 3rd Revised Edition.* Springer-Verlag, New York, New York, USA.

PARK C. S., NEWFIELD M. E., FLETCHER D. G., GÖKÇEN T. AND SHARMA S. P. (1997) Spectroscopic emission measurements within the blunt-body shock layer in an arc-jet flow. AIAA 97-0990, 35th Aerospace Sciences Meeting and Exhibit, Reno, Nevada, USA.

PARK C. S., NEWFIELD M. E., FLETCHER D. G., GÖKÇEN T. AND SHARMA S. P. (1998) Spectroscopic emission measurements within the blunt-body shock layer in an arcjet flow. *J. Thermophyis. Heat Transfer* **12**, 190–197.

POPOVA O. P., SIDNEVA S. N., SHUVALOV V. V. AND STRELKOV A. S. (2000) Screening of meteoroids by ablation vapor in high-velocity meteors. *Earth, Moon Planets* **82–83**, 109–128.

RAIRDEN R. L., JENNISKENS P. AND LAUX C. O. (2000) Search for organic matter in Leonid meteoroids. *Earth, Moon Planets* **82–83**, 71–80.

RIETMEIJER F. J. M. AND NUTH J. A. (2000) Collected extraterrestrial materials: Constraints on meteor and fireball compositions. *Earth, Moon Planets* **82–83**, 325–350.

STEVENS M. H., CONWAY R. R., ENGLERT C. R., SUMMERS M. E., GROSSMAN K. U. AND GUSEV O. A. (2001) PMCs and the water frost point in the Arctic summer mesosphere. *Geophys. Res. Lett.* **28**, 4449–4452.

YEOMANS D. K., YAU K. K. AND WEISSMAN P. R. (1996) The impending appearance of Comet Tempel–Tuttle and the Leonid Meteors. *Icarus* **124**, 407–413.